Adaptive Controller PI-Fuzzy logic Speed for Brushless DC Motor Drive Supplied by PEMFC Cell Optimized by P&O

YAMINA JOUILI, RADHIA GARRAOUI, MOUNA BEN HAMD, LASSAAD SBITA

Dept. Electric-Automatic, University of Gabes, Gabes, TUNISIA
National Engineering School of Gabes, Omar ibn elkatab Road, Gabes, 100190, TUNISIA

Abstract: - Brushless Direct Current (BLDC) motors have recently gained momentum. In this study, a fuel cell stack, namely, a Proton-Exchange Membrane Fuel Cell (PEMFC), one of the promising renewable energy technologies, is chosen for a brushless DC motor. To improve the performance of PEMFC, an efficient maximum power point tracking (MPPT) algorithm was applied to the DC/DC boost converter. To this end, the perturbation and observation (P&O) algorithm were developed. This work proposes an adaptive controller proportional-integral (PI)-fuzzy logic speed for the BLDC. To evaluate its performance, the proposed controller was simulated under several conditions: load disturbance and reference speed variation. This controller is analyzed and compared with the classical PI controller. Therefore, the control performance parameters, such as rise time, settling time, steady-state error, and overshoot, were determined and compared. This system is analyzed and simulated using MATLAB/Simulink software.

Key-Words: - PEMFC, P&O, Adaptive PI-FL controller- PI - BLDC.

Received: September 22, 2022. Revised: May 23, 2023. Accepted: June 19, 2023. Published: July 17, 2023.

1 Introduction

Today, the world is becoming aware of the problems associated with traditional energy sources that have destructive impacts on the environment, such as fossil fuels and non-renewable energy sources.

Fuel cells are a potential alternative energy source to fossil fuel-based power generators for clean electricity production. Recently, this technology has attracted much attention in electrical energy generation, namely electric vehicles, mobile robots, and unmanned aerial vehicles (UAVs) [1-3].In addition, the fuel cell is not burned: the energy is produced by an electrochemical reaction. It can provide continuous energy in all seasons, providing that fuel is available [4].

PEMFCs are the most popular and can operate at low temperatures below 100°C. They are commercially available, with high efficiency (up to 50%), fast start-up, as well as high reliability with no pollution.

However, fuel cell systems have problems related to harvesting electrical energy from the PEM FC stack. FC systems have nonlinear output characteristics because of their input variation, which causes a significant loss in the overall system output.

So, an MPPT algorithm must be developed to enhance and optimize the PEMFC system efficiency. The problem of fuel starvation resulting from sudden changes in load can cause severe damage to the fuel cell membrane.

Many studies have addressed control problems related to PEMFCs in the last few years, and diverse control techniques have been used. During the last few decades, many studies have addressed control problems related to PEMFC. For instance, authors of [1] proposed a smart MPPT algorithm based on FLC.

Further, this type of fuel cell has been used as the primary power source in rotary actuators. Many studies have investigated the possibility of powering electric motors with hydrogen technologies [2].

Hence, in this study, to improve power quality, system performance, and design optimization, the PEMFC system needs to be modeled and analyzed.

At present, electric rotary actuators play a crucial role in commercial and residential applications. The DC motor has been used mostly in actuators [1]. However, its main drawback remains the mechanical commutator, which causes brush wear and rotor losses, the susceptibility of the commutator, the consequent need for maintenance, lower robustness, and the need for more expensive control electronics [4].

Due to their favorable electrical and mechanical properties, Brushless Direct Current **(**BLDC) motors are found in several segments, mainly in variable speed operations, such as an unmanned aerial vehicle (UAV), robotics, electric vehicles, and electromechanical actuation systems [6].

BLDC motors belong to the synchronous motor type with an electric commutation scheme. These drives have become the best choice due to continuous improvements in high-energy permanent magnet materials, power semiconductors, and digital integrated circuits [7, 8]. Thus, a BLDC motor has a high power-to-mass ratio, less maintenance, and high-speed capabilities [9-11]. Various control schemes are created for speed regulation in a closed loop, such as the Proportional Integral Derivative (PID), optimization of PI coefficients using Genetic Algorithm (GA), Fuzzy Logic Controller (FLC), and Adaptive tuned Fuzzy Logic [12, 13].

PI controllers are widely used in industrial control systems and several other applications that need modulated control due to their simplicity of adjustment and regulation. Conventional PID controllers have become inefficient as they are non-linear systems due to unstable conditions, higher order, complexity, and having no mathematical model.

To overcome these shortcomings, previous works have focused on adaptive control; for example, an adaptive PID neural network controller is developed in [14-17]. Moreover, the particle swarm optimization (PSO) algorithm was used for controller design. However, it takes a higher time delay to initialize the weight of the PID neural network. An adaptive neuro-fuzzy inference System (ANFIS) was developed in [18-20]. This controller enhances the steady-state speed response but degrades the transient response and is trained in offline tuning. Besides, a self-adaptive PID-fuzzy logic controller has been proposed for speed control by several research works [21-23]. As such, fuzzy logic control is used in online gains tuning. Furthermore, the intelligent control techniques are applied to dynamic systems guaranteeing high robustness performance with a better steady-state response, short rise and settling times, and low overshoot.

In this study, all the performance factor parameters of control are measured for the proposed controllers, namely adaptive PI-FL, and compared with the classical proportional-integral (PI) controller,

The remainder of the paper is organized as follows: Section 2 describes the dynamics of the PEMFC stack with the Maximum Power Point Tracking (MPPT) strategy based on the Perturb and Observe (P&O) method. Then, the mathematical models of the BLDC engine are developed in Section 3, and the proposed controllers are explained in Section 4. The simulation results are illustrated and discussed in the next section. Section 6 concludes the paper.

2 Modeling of PEMFC

A fuel cell is an electrochemical energy conversion device capable of converting chemical energy into electrical energy [24, 25]. The proposed system uses a PEM fuel cell as a power supply source. This device consists of an anode and a cathode supplied with hydrogen and oxygen. These electrodes are separated by an electrolyte and two catalysts, usually made of platinum, as shown in Fig.1 [26-28]. Hydrogen is the anodic reactant releasing two electrons and the ion H+ according to equation (1). Oxygen is the cathodic reactant or oxidant, as indicated in equation (2). The working principle of PEMFC is based on the anode oxidation of

hydrogen (fuel) to protons. This process generates electrical energy and hot water, as in equation (3).

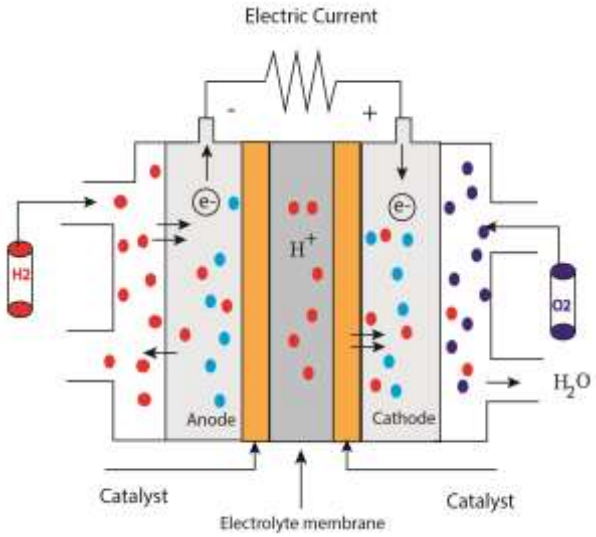

Fig.1. chemical reactions of the fuel cell.

The electrochemical reactions occurring at the electrodes of the PEMFC are described by the following equations:

Anode reaction

$$H_2 \rightarrow 2H^+ + 2e^- \quad (1)$$

Cathode reaction

$$2H^+ + \frac{1}{2}O_2 + 2e^- \rightarrow H_2O \quad (2)$$

The full reaction in the PEM fuel cell produces electricity, water, and heat as follows:

$$H_2 + \frac{1}{2}O_2 \rightarrow H_2O + heat + energy \quad (3)$$

According to [25] and [29], the PEM fuel cell is calculated from the electrochemical reactions expressed by the Nernst equation as follows:

$$V_{cel} = E_{Nernst} - V_{act} - V_{\Omega} - V_{con} \quad (4)$$

Where the first term is the thermodynamic potential of the cell representing its reversible voltage (without load) as:

$$E_{Nernst} = 1.229 - 0.85.10^{-3}\left(T - 289.15\right) + 4.31.10^{-5}.T\left(Ln(Ph_2) + 0.5Ln(Po_2)\right) \quad (5)$$

T represents the cell temperature, Ph2 is the partial pressure of hydrogen, and Po2 is the partial pressure of oxygen at the catalyst gas.

While the three last terms, V_{act}, V_{Ω}, and V_{con}, represent the voltage losses; thus, voltage drops or over potential caused by reaction activation, ohmic resistances, and gas diffusion are given by equations (6) to (8):

$$V_{act} = \xi_1 + \xi_2.T + \xi_3.T.Ln(Co_2) + \xi_4.T.Ln(i) \quad (6)$$

ζi represents the parametric coefficients for each cell, i is the cell operating current, and Co2 is the concentration of oxygen gas in the catalytic cathode.

$$V_{con} = -B.Ln\left(1 - \frac{J}{J_{max}}\right) \quad (7)$$

Where B is the parameter influent by cell type, J_{max} is the maximum current density, and J represents the actual current density of PEMFC.

$$V_{\Omega} = i.\left(Rc + Rm\right) \quad (8)$$

Rc is proton resistance, taken as a constant value, and Rm represents the equivalent membrane resistance of the electron.

CO2, J, and Rm of the PEM fuel cell mathematical model are presented in [4] and [10].

In an elementary cell, the nominal voltage is about 0.8 V, and the current density can reach 1A /cm^2. The output current is proportional to the active area. Because the voltage is too low to directly connect a power converter to achieve the required voltage levels for larger-scale applications, several cells must be connected in series to form a stack.

The mathematical model of the PEM fuel cell was simulated under (MATLAB/Simulink) environment. Moreover, a step-up converter (DC/DC) was used for voltage regulation. The MPPT controller generator was used to drive the Pulse Width Modulation (PWM) of the converter

device, and the Simulink model for the fuel cell stack is shown in Fig.2.

Therefore, the fuel cell stack voltage response is given by:

$$V_{PEMFC} = N.\left[E_{Nernst} - V_{act} - V_{\Omega} - V_{con}\right] \quad (9)$$

Where N represents the number of fuel cells in the stack

The mathematical model of the PEM fuel cell was simulated under (MATLAB/Simulink) environment. Moreover, a step-up converter (DC/DC) was used for voltage regulation. The MPPT controller generator was used to drive the Pulse Width Modulation (PWM) of the converter device.

2.1 The boost converter

The circuit configuration of the boost converter (DC/DC) is depicted in Fig. 2. It consists of a DC source, an inductor L, a filter capacitor C, a load resistor R, a transistor T, and a diode D [21]. The gate pulses to control the switches S. The converter's operating modes are represented as follows:

First, the inductor current increases when the switch S is on (S=1). The voltage inductor is the voltage input to the circuit as:

$$\begin{cases} \frac{dI_{fc}}{dt} = \frac{1}{L} V_{in} \\ \frac{dV_{out}}{dt} = \frac{1}{C}(-I_{out}) \end{cases} \quad (10)$$

Second, when S is off (S=0), the energy accumulated is transferred into the capacitor. The voltage of this state is calculated by (11):

$$\begin{cases} \frac{dI_{fc}}{dt} = \frac{1}{L}.V_{in} - \frac{1}{L}.V_{out} \\ \frac{dV_{out}}{dt} = \frac{1}{C}(I_{fc} - I_{out}) \end{cases} \quad (11)$$

According to the position of the switch S, the dynamic system of the boost converter circuit can be written as:

$$\begin{cases} \frac{dI_{fc}}{dt} = \frac{V_{in}}{L} - (1-\alpha)\frac{V_{out}}{L} \\ \frac{dV_{out}}{dt} = (1-\alpha).\frac{I_{fc}}{C} - \frac{1}{C}.I_{out} \end{cases} \quad (12)$$

Where V_{out} represents the output voltage of the load, V_{in} is the input voltage from the cell stack, and α is the signal control that defines the switch position.

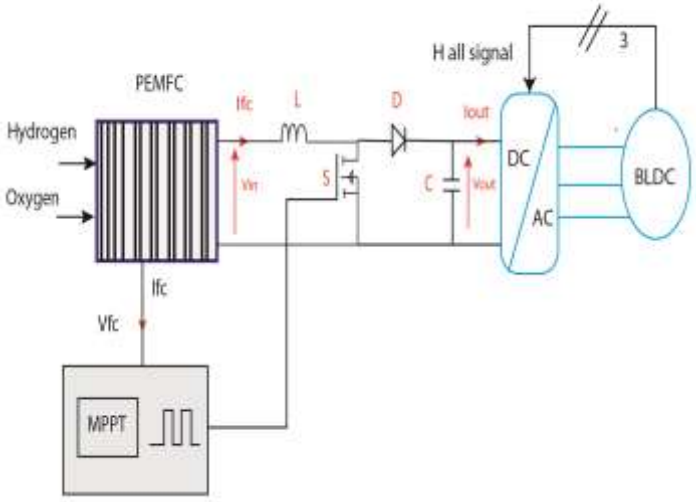

Fig.2: Schematic of the proposed system.

2.2 MPPT design

In the proposed scheme, the P&O algorithm of the MPPT strategy is realized to maximize the PEMFC outturn. The MPPT control strategy is based on changing the converter's duty cycle to force the cell stack to operate at adequate power [29-30]. This algorithm works by periodically perturbing the Ifc and observing the resulting change in power output. Indeed, the MPPT algorithm is started by calculating the power at zero amperes. Then, the cell stack (PEMFC) voltage and current are perturbed slightly, and a new power value is calculated. The P&O algorithm is illustrated in Fig.3.

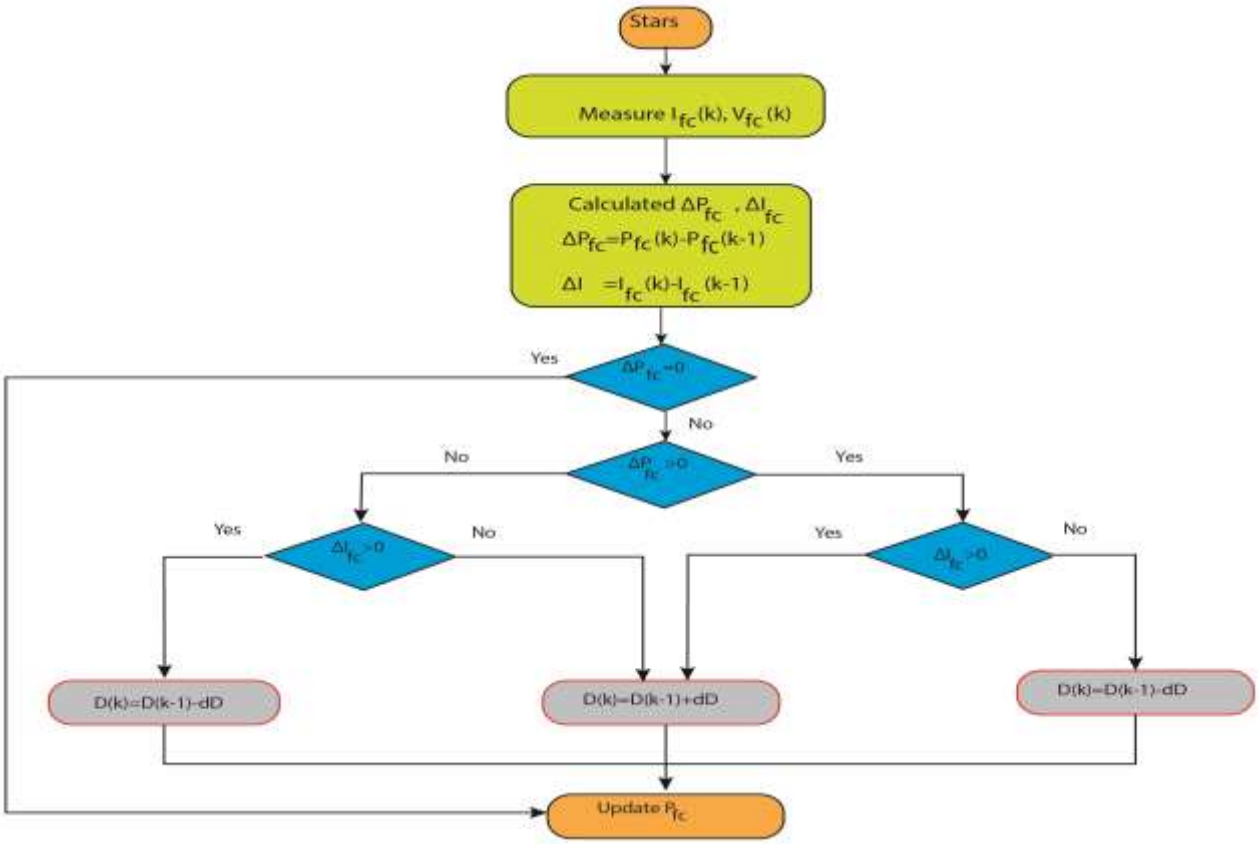

3 BLDC motor description and modeling

Unlike the DC machine, the Brushless motor does not use brushes for commutation. The BLDC consists of a permanent magnet that replaces the coil and does not require brushes; thus, noise, interference, and graphite dust could be avoided. It uses an electronic controller for switching DC currents in the winding stator [31]. A DC/AC inverter is used for this purpose. The phase current of the BLDC motor, typically with a rectangular waveform, is synchronized with the back-EMF to produce a constant torque at a constant speed. Thus, there are two strategies of control systems: sensored and sensorless. The latter reduces the cost of the BLDC; however, finding the Back-EMF for low-speed applications is problematic.

A BLDC motor is usually modeled as a series connection of a stator winding resistance, an inductance, and a counter-electromotive force (CEF) (Fig.4).

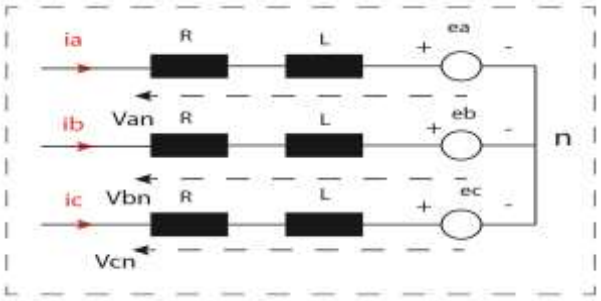

Fig.4. Equivalent circuit of BLDC

Mathematically, the brushless DC motor model is similar to that of a conventional DC motor [31, 32]. The stator phase currents are a balanced system. The output voltages of the BLDC motor can be described by matrix equations (13).

$$\begin{bmatrix} V_a \\ V_b \\ V_c \end{bmatrix} = \begin{bmatrix} R & 0 & 0 \\ 0 & R & 0 \\ 0 & 0 & R \end{bmatrix} . \begin{bmatrix} i_a \\ i_b \\ i_c \end{bmatrix} + \begin{bmatrix} L-M & 0 & 0 \\ 0 & L-M & 0 \\ 0 & 0 & L-M \end{bmatrix} . \frac{d}{dt} . \begin{bmatrix} i_a \\ i_b \\ i_c \end{bmatrix} + \begin{bmatrix} e_a \\ e_b \\ e_c \end{bmatrix} \quad (13)$$

Where V_{abc} are the three-phase stator voltages of the brushless dc motor drive, R, L, and M represent the stator resistance, self-inductance, and mutual inductance of winding, respectively. i_{abc} signifies the three-phase currents of the BLDC motor, and the back electromotive forces (e_{abc}) are expressed by equation (14).

$$\begin{cases} ea = \frac{k_e}{2}.\dot{\theta}_m.F(\theta_e) \\ eb = \frac{k_e}{2}.\dot{\theta}_m.F\left(\theta_e - \frac{2\pi}{3}\right) \\ ec = \frac{k_e}{2}.\dot{\theta}_m.F\left(\theta_e - \frac{4\pi}{3}\right) \end{cases} \quad (14)$$

K_e represents the back-emf constant. Electrical and mechanical angles are represented by θe and θm:

$$\theta e = p.\theta m \quad (15)$$

With p is the pairs of poles, and F(.) is the function that gives the trapezoidal of the back EMF described as follows:

$$F(\theta_e) = \begin{cases} 1 & 0 \le \theta_e \le \frac{2\pi}{3} \\ 1 - \frac{6}{\pi}.\left(\theta_e - \frac{2\pi}{3}\right) & \frac{2\pi}{3} \le \theta_e \le \pi \\ -1 & \pi \le \theta_e \le \frac{5\pi}{3} \\ -1 + \frac{6}{\pi}.\left(\theta_e - \frac{5\pi}{3}\right) & \frac{5\pi}{3} \le \theta_e \le 2\pi \end{cases}$$

(16)

The mechanical movement equation can be expressed as follows:

$$T_{em} = \frac{1}{J}\frac{d\omega_m}{dt} + \beta.\omega_m(t) + T_L(t) \quad (17)$$

Where J represents the moment of inertia, β is the frictional constant, and TL is the load torque.

Since the electromagnetic torque of the three-phase BLDC can be represented by the back emf, three-phase current, and speed, the equation for electromagnetic torque is modified and represented as follows:

$$T_{em} = \frac{e_a.i_a + e_b.i_b + e_c.i_c}{\dot{\theta}_m} \quad (18)$$

Fig.5 depicts a Simulink model in the inner loop [34].

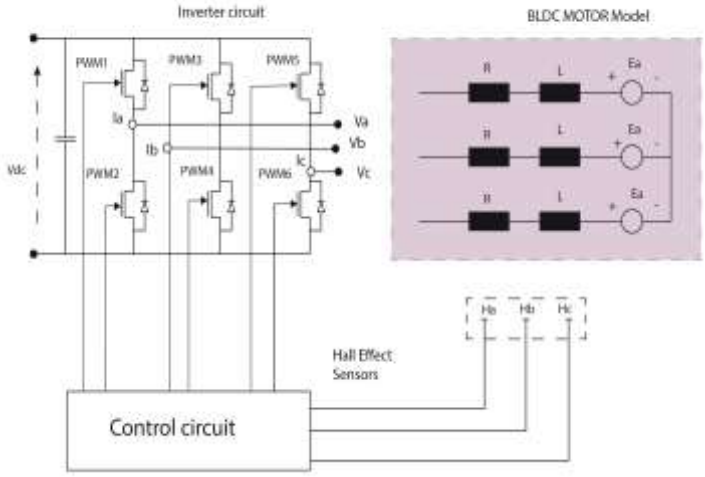

Fig.5: BLDC motor in open loop.

4 Controller design of a BLDC motor

The overall control strategy for the brushless dc motor is developed with MATLAB/Simulink software. Fig.6 displays the considered Simulink model blocks, such as the BLDC motor, dc bus, inverter device, current control block (inner loop), speed control block (outer loop), and motor measurement block.

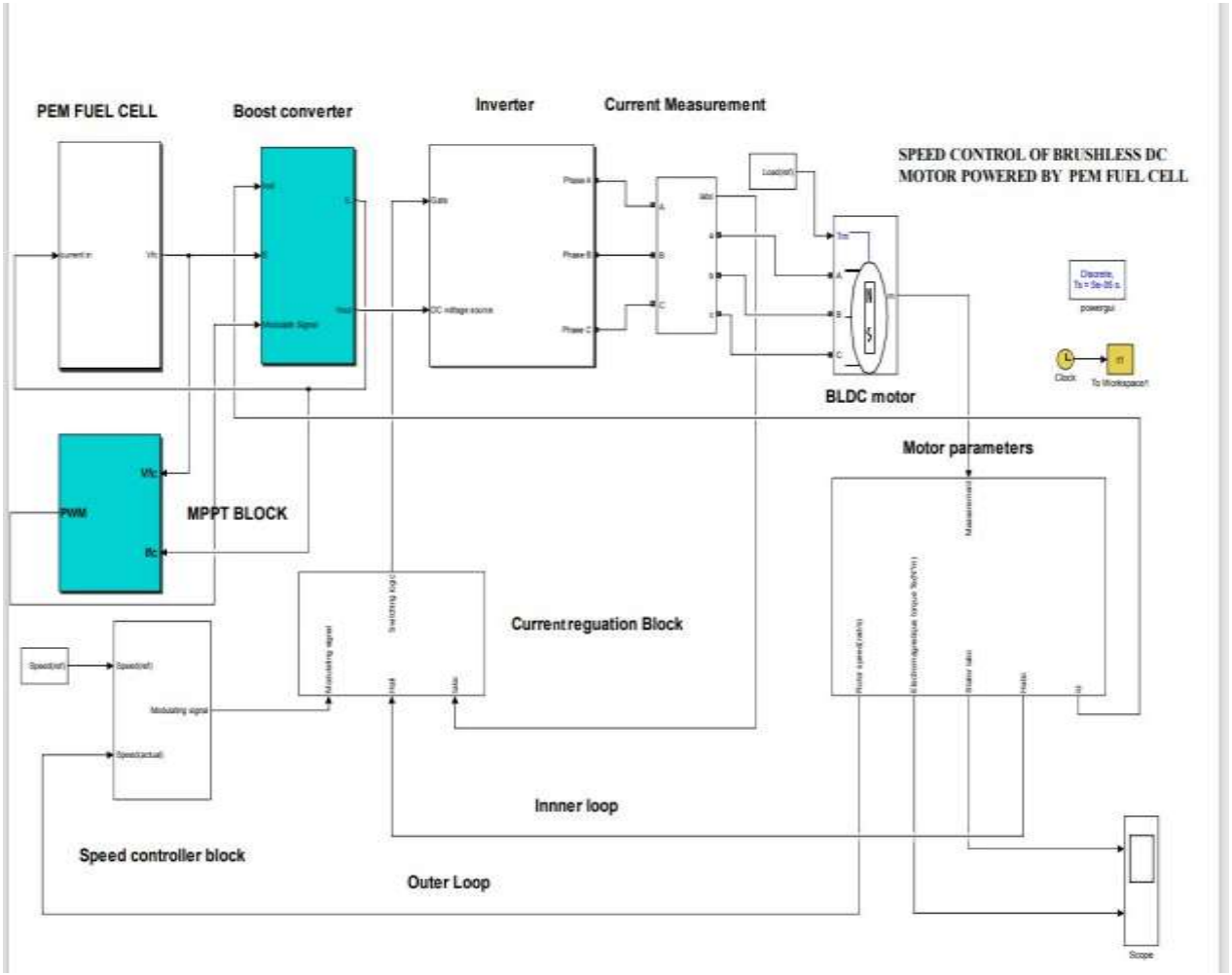

Fig.6: Simulink model blocks of the proposed controller for BLDC motor.

4.1 Current regulation

Duty-cycle controlled voltage PWM technique and hysteresis current control technique are effective methods in improving the performance of current control strategies for a BLDC.

In the present work, the hysteresis current controller is chosen to generate the necessary PWM signals for the inverter and obtain fast dynamic responses during transient states. This method is used to replace the voltage control in BLDC. In this control technique, the value of the controlled variable is forced to stay within certain limits [33]. Therefore, the reference current generator is determined by the reference torque using the following expression:

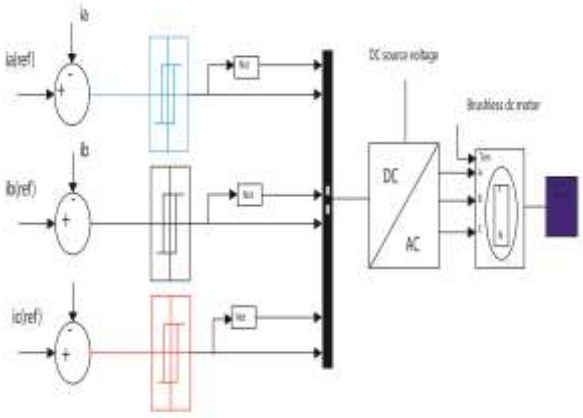

Fig.7: Hysteresis current regulation block

$$i_{a,b,c_{ref}} = \frac{T_{ref}}{Kt} \quad (19)$$

with Kt is the torque constant.

Table. 1. Decoder Signals based on Hall Effect sensor states

Hall effect sensor			Decoded Signals		
Ha	Hb	Hc	Ea	Eb	Ec
0	0	0	0	0	0
0	0	1	0	-1	+1
0	1	0	-1	+1	0
0	1	1	-1	0	+1
1	0	0	+1	0	-1
1	0	1	+1	-1	0
1	1	0	0	+1	-1
1	1	1	0	0	0

4.2 Speed regulation

In what follows, we will study speed regulation. To enhance the BLDC motor performance, two control methods are developed. Firstly, a classical PI controller is used. Secondly, a self-adaptive PI approach is designed to control the speed of the BLDC motor. On the one hand, it benefits from the advantages of the PI controller, such as feasibility, simplicity, easy implementation, and performance. In particular, the performance of this technique is significant in autonomous systems. On the other hand, the gains of this controller are adjusted by an online optimization method with a fuzzy logic strategy.

Self-adaptive PI-Fuzzy logic control

Unfortunately, the PI gains must be balanced to improve the transient response and, thus, the performance parameters of the system, such as the settling time, overshoot, oscillation, and steady-state error, under various operating conditions. However, in the event of poor estimation or constant gain values, the control system parameters suffer due to uncertainties and disturbances in the operating conditions of the brushless dc motor. Practical experiments have shown that the PI or PID controller design could be optimized by the fuzzy logic controller so that the control performance of the controller could be enhanced with better stability and high robustness.

In this paper, self-adaptive PI-fuzzy logic would have to decide and allow changing the gains online. On the one hand, the adaptive PI-FL controller enjoys the advantages of the PI controller, such as feasibility and easy implementation.

On the other hand, the fuzzy logic controller (FLC) is known for its capability to handle different output sets depending on the input, which is ideal for a non-linear system without the requirement of its mathematical model.

FLC mainly comprises fuzzification, inference fuzzy rule base, and defuzzification as elemental components. In this work, a fuzzy inference system with the Sugeno model is proposed for the tuned PI (adaptive PI-FL) controller. It depends mainly on the value of update gains, speed error e, and its rate of change ec as the fuzzy logic controller inputs. Two output signals, kp, and ki are given to produce the desired control The input variables are to be fuzzy sets, such as PL (positive low), PH (positive high), Z (zero), NL (negative low), and NH (negative high). In addition, the output signals are distributed with three membership functions that describe the linguistic variables Z (zero), L (low), and M (medium). The used membership functions of FL control are described in the Figures below.

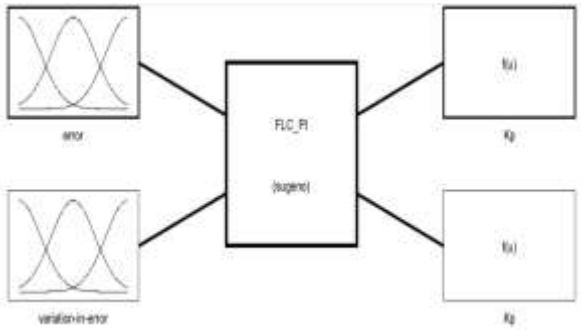

Fig.8: Proposed FLC controller.

		ΔE				
	Kp	**NH**	**NL**	**Z**	**PL**	**PH**
E	**NH**	**L**	**L**	**Z**	**L**	**L**
	NL	**L**	**L**	**M**	**L**	**L**
	Z	**L**	**L**	**M**	**L**	**L**
	PL	**L**	**L**	**M**	**L**	**L**
	PH	**L**	**L**	**L**	**L**	**L**

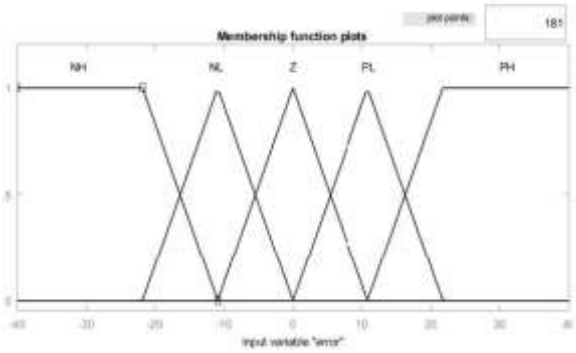

Fig.9: Distribution of membership functions for of error speed.

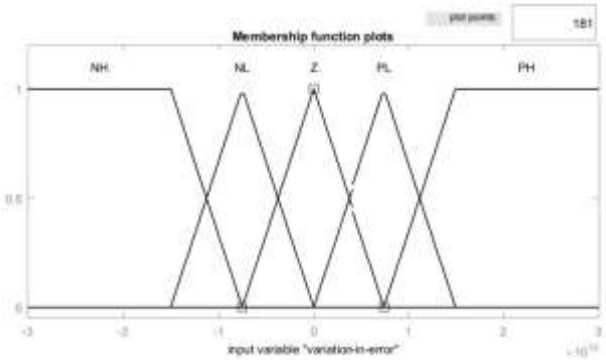

Fig.9: Distribution of membership functions for of error speed.

Through fuzzification and fuzzy decision, overall, the outputs are given in Table 2 and 3. Here, 25 fuzzy

Control rules are produced. Each of them is obtained from the "IF-THEN" interference rules. In control theory, the set of rules can be separated into four groups to achieve the logic of the proposed rules. In group 1: the velocity error and the rate of change error of the velocity have zero, small negative, or positive values. In this case, the velocity output is slightly below or above the set points. Therefore, small negative or positive control values are applied.

As proposed, the kp update values are zero or low, while the ki update values are zero or medium. In group 2: the velocity error and the rate of change error of the velocity have negative or positive values. For this group, negative control values are required for optimal operation, and the process output is far below the set point. In this case, the online kp fuzzy sets have medium, but the online ki fuzzy sets have low, or zero values.

Table.2: The decision of the fuzzy inference rules of kp

		ΔE				
	Kp	**NH**	**NL**	**Z**	**PL**	**PH**
E	**NH**	**M**	**M**	**L**	**M**	**M**
	NL	**M**	**M**	**M**	**M**	**M**
	Z	**Z**	**Z**	**Z**	**Z**	**Z**
	PL	**M**	**M**	**L**	**M**	**M**
	PH	**M**	**M**	**M**	**M**	**M**

Table.3: The decision of the fuzzy inference rules of ki

Table.4: Parameters of bldc motor

Name	Value	Value
viscous damping	0.005	N.m.s
Inertia	0.089	Kg.m^2
pole pairs	8	-
static friction	0	N.m
Stator phase resistance	0.2	Ω
Stator phase inductance Ls	8.5e-3	H
Torque constant	1.4	N.m/A_peak

5 Simulation Results

PI and adaptive PI-FL controllers were previously developed for brushless DC motors. To achieve the optimal control strategy, several states were simulated from different load states and different set point speed states. These controller designs were then compared to obtain control performance parameters, such as rise time, settling time, steady state error, overshoot, and undershoot. The results were obtained using MATLAB/Simulink software; the global specification of the brushless DC motor is shown in Table 4. Fig 10 shows the block diagram for the identifier. The actual speed of the BLDC motor will be compared with the reference speed to obtain the error signal and rate of change of error.

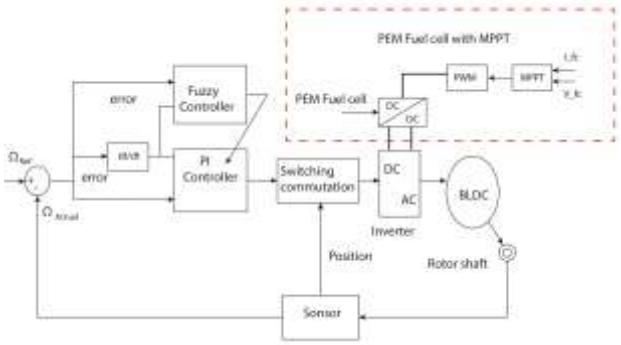

Fig.10: Blocks of the proposed system

The operating performance of an individual cell is shown in Fig.11. Thus, they depend on the three main polarization losses: activation, ohmic, and concentration losses. First, it starts from the maximum voltage of the cell, then it behaves linearly, and finally, a sudden drop occurs at a higher current density. As can be seen from Fig 12, the power received from the FC is 203.8 W, the voltage is 24.23 V, and the current is 8.55 A. This fuel cell consists of 40 cells. This stack runs at a temperature of 298.15 K and pressure of (1.486 atm and 0.98 atm).

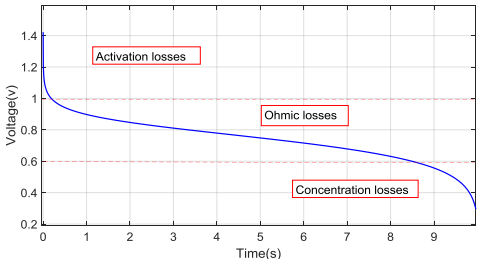

Fig.11: Polarization curve of the PEM fuel cell

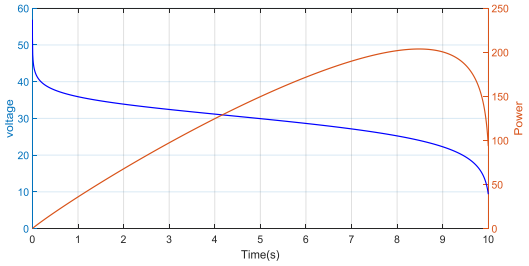

Fig.12: PEMFC generator characteristics.

The proposed MPPT technique works efficiently and tracks the optimal performance of the fuel cell stack, as shown in Fig.13 a, b, and c. The curves show respectively, the PEMFC output of power, the duty cycle signal, and boost converter output signals (voltage and power). These curves show the

behavior of the MPPT strategy (P&O) to maintain and track the optimal performance of the PEMFC stack.

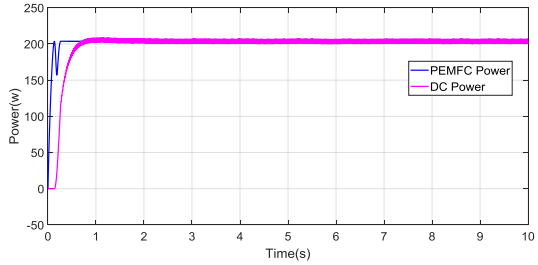

(a)

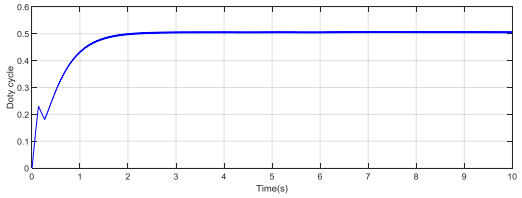

(b)

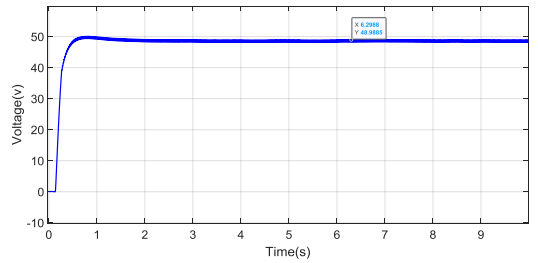

(c)

Fig.13: Responses for constant condition, (a) DC link power and power of PEMFC generator, (b) duty cycle response, (c) DC voltage response.

The phase currents, torque, and back EMF of the BLDC motor are also shown in the following figures. The observed ripple in the current waveforms is due to the use of the PWM method for the speed control of the BLDC motor. Acceptable ripples occurred on the motor torque curves. The current values change with the torque value. So, The square waveforms of phase currents verify the good control capability of the BLDC motor for all three conditions.

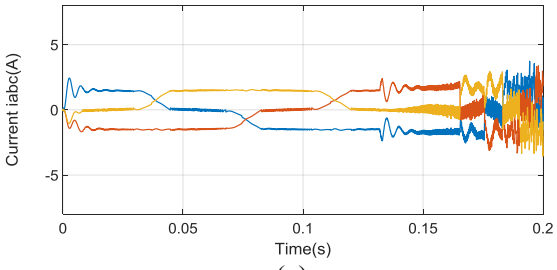

(a)

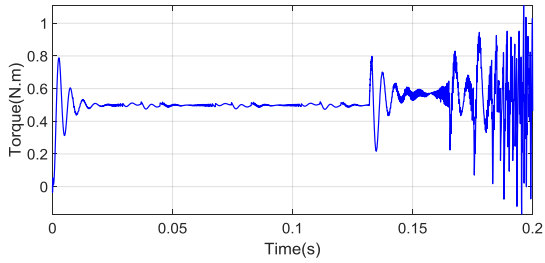

(b)

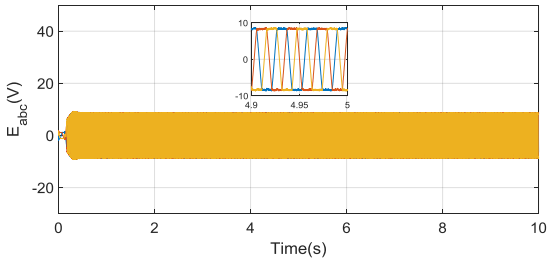

(c)

Fig.14: Brushless dc motor response, a) phase current waveforms, b) torque waveform, c) stator back EMF_{abc}

Adaptative PI-FL (fuzzy-tuned PI) controller is modeled using sugeno's method with a constant value, having two inputs and two outputs. The Update values of online gains are multiplied by velocity error. Then, the control signal (U) is used to adjust the system. Simulation results of the speed response of the BLDC motor with classical PI and fuzzy-tuned PI controller are shown in Fig.15.

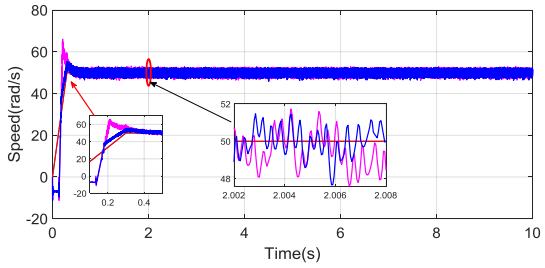

Fig.15: speed response for constant variation condition

The results were obtained by keeping the reference speed at 50 rad/s and the load torque constant at 0.5Nm. From the above speed plots, the fuzzy-tuned PI and PI controllers reach the reference set speed with a rise time equal to 0.237. The fuzzy-tuned PI manifests overshoot

and undershoot speeds of 0.0934 (%) and 0(%), respectively. The PI controller displays overshoot and undershoots speeds of 0.3204 (%) and 0(%), respectively. For the same variations, the fuzzy-tuned PI shows a settling time and steady-state error of 0.3875 (s) and -0.210(rad/s), respectively. The PI controller has a settling time and steady-state error of 0.4035 (s) and -0.4808 (rad/s), respectively. In addition, the performance parameter values of the controllers are illustrated in Table 5.

Table 5: Comparison of performance parameters for constant condition

Controller	Control performance parameters						
	Rise time (s)	Peak time (s)	Peak value (rad/s)	Overshoot value (%)	Undershoot (%)	Settling time (s)	steady-state error(rpm)
PI	0.1878	0.212	66.02	0.3204	0	0.4035	-0.4808
PI-Fuzzy logic	0.237	0.2989	54.67	0.0934	0	0.3875	-0.2100

5.1 Results under load variation

The brushless DC motor must operate under varying load conditions in most industrial applications. To evaluate the performance of the proposed controller, the closed-loop system of the brushless DC motor is operated with load variation. The load increases from 0.5 to 0.9Nm at t= 5s (Fig.16).

Fig.17,(a) and (b),(c), and (d) show the simulation results obtained for varying load conditions. The performance comparison of the proposed controllers is shown in table 6. We consider control performance parameters, such as rise time, overshoot, settling time, peak time, peak value, and undershoot, as comparison factors. Fig.17 (a) and (b) illustrate the online gain value of the FL control and Figure.17 (c) and (d) describe the duty cycle of MPPT strategy and speed response of BLDC behaviour under the same conditions.

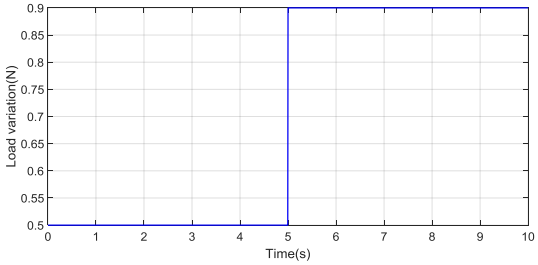

Fig.16: Load variation

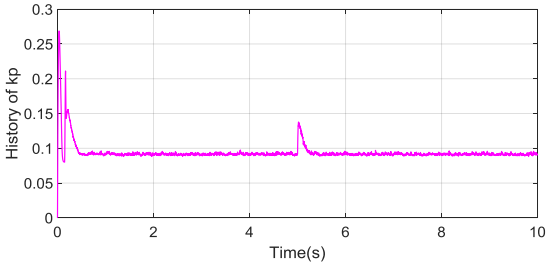

(a)

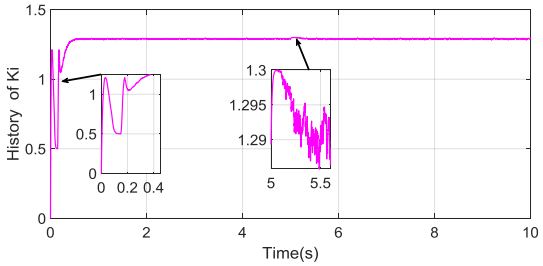

(b)

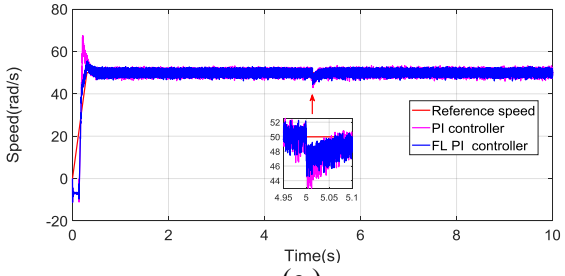

(c)

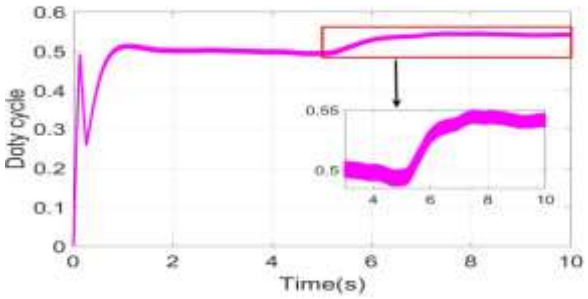

(d)

Fig.17: Responses for load variation condition and online control parameters, a) Kp, b) ki, c) Duty cycle, d) speed of BLDC motor.

Consequently, the proposed Fuzzy-tuned PI controller for the brushless dc motor drive is perfectly tracked, and its oscillations are effectively improved. When the load is increased, the proposed controller restores the system to the set value in the shortest possible time and produces a low undershoot value. Then, the comparison of the numerical performance of the controllers is given in Table 6.

5.2 Results under speed variation

At the same time, the BLDC motor may be required to operate at variable speed conditions. To validate the effectiveness of the proposed controller, the speed response is obtained under varying speed conditions. In the first case, the step reference speed is varied from 50 to 90 rad/s and then from 90 to 50 rad/s, applied at time t= 4s and 7s (Fig.19). The proposed speed operating conditions are simulated, and the curves of speed responses are displayed in figure 20,(d). In addition, the FL control online value of gain for kp and ki under the same conditions is shown in figure 20, (a) and (b). Figure.21, (c) represents the duty cycle of the MPPT algorithm. Then, the comparison of the numerical performance of the controllers is illustrated in table 7.

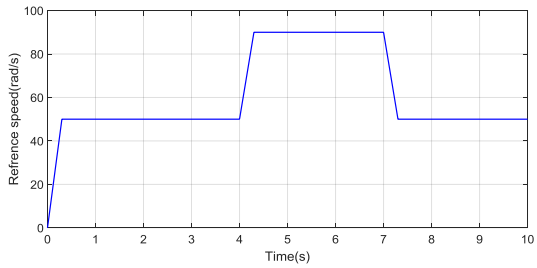

Fig.19: Speed variation

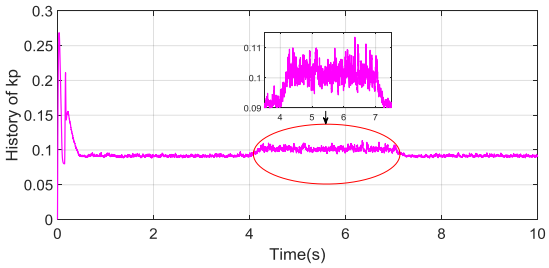

(a)

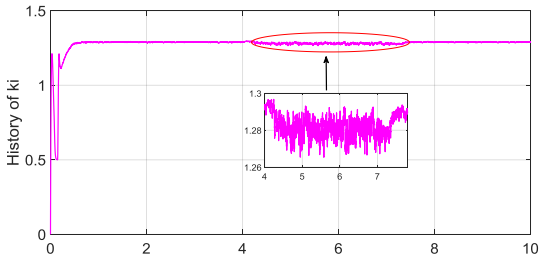

(b)

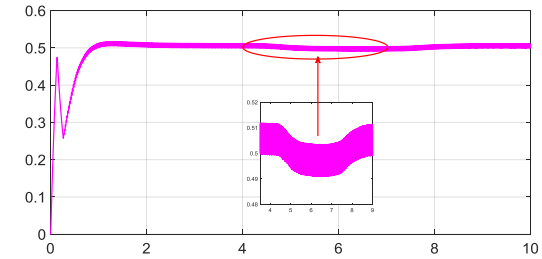

(c)

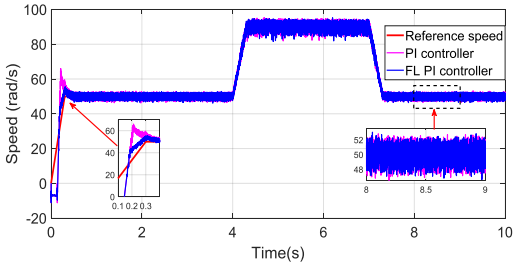

Fig.20: System responses for speed variation and online control parameters, a) Kp, b) ki, c) Duty cycle, d) speed of BLDC motor

Table 6: Comparison of performance parameters for load variation conditions

Controller	Control performance parameters						
	Rise time (s)	Peak time (s)	Peak value (rad/s)	Overshoot value (%)	Undershoot (%)	Settling time (s)	steady-state error(rpm)
PI	0.196	0.2119	67.08	0.3416	0.1404	0.3947	-1.0886
PI-Fuzzy logic	0.2289	0.2985	55.11	0.1022	0.1080	0.3392	0.3621

Table 7: Comparison of performance parameters for speed variation conditions

Controller	Control performance parameters						
	Rise time (s)	Peak time (s)	Peak value (rad/s)	Overshoot value (%)	Undershoot (%)	Settling time (s)	steady-state error(rpm)
PI	0.191	0.2119	67.08	0.3416	0	0.427	-0.6578
PI-Fuzzy logic	0.209	0.3137	55.54	0.1108	0	0.3772	-0.6337

Simulation results and comparison tables show that the proposed controller for BLDC performs very well under speed and load variation conditions. Small oscillations of the speed curve are observed following the application of the Fuzzy tuned PI controller in both cases. Moreover, the rotor speed follows perfectly its speed reference but with some differences depending on the type of controller applied.

6 Conclusion

To achieve an accurate MPPT of the PEM fuel cell, the P&O strategy was proposed by controlling the DC/DC boost converter. Considering a more reliable and simpler controller, a self-adaptive PI-Fuzzy logic controller was used with the brushless dc motor under load disturbance and reference speed variation. To this end, the proposed controller

was compared with the classical PI controller. Thus, the performance parameters of the controller, such as rise time, peak time, peak value, overshoot, undershoot, settling time, and steady-state error was measured and presented. Based on the obtained simulation results and analyses performed in this work, the following conclusions can be
drawn:

- The proposed MPPT design technique works efficiently, tracks the optimal performance of the fuel cell stack, and maintains a constant current for sudden external disturbance.

- The proposed controller for the BLDC works very well. It has a low oscillation of the speed curve for varying conditions.
- The proposed controller improved the performance of the controller parameters compared to the conventional PI controllers in terms of minimum rise time, settling time (s), and steady-state error value under all operating conditions.

The proposed controller can eliminate the uncertainty problem due to load and speed variations. Since the controller has high performance, it is ideal for the processing industries. The selection of fuzzy logic parameters, such as fuzzy membership functions, fuzzy rules, and inputs and outputs, can limit the proposed controllers' performance. Optimization algorithms that can be applied for the selection and tuning of fuzzy logic parameters to achieve efficient results under different circumstances will represent avenues for future research works.

References:

[1] Derbeli, M.; Sbita, L.; Farhat, M.; Barambones, O. Proton exchange membrane fuel cell—A smart drive algorithm. *In Proceedings of the 2017 International Conference on Green Energy Conversion Systems (GECS),* Hammamet, Tunisia, 23–25 March 2017; pp. 1–5. [CrossRef]

[2] Derbeli, M., Barambones, O., Ramos-Hernanz, J. A., & Sbita, L. (2019). Real-time implementation of a super twisting algorithm for PEM fuel cell power system. *Energies*, 12(9), 1594. https://doi.org/10.3390/en12091594.

[3] Souissi, A. (2021). Adaptive sliding mode control of a PEM fuel cell system based on the super twisting algorithm. *Energy Reports*, 7, 3390-3399. https://doi.org/10.1016/j.egyr.2021.05.069.

[4] Schumann, M., Grumm, F., Friedrich, J., & Schulz, D. (2019). Electric field modifier design and implementation for transient pem fuel cell control. *WSEAS transactions on circuits and systems*

[5] Xing, L., Xiang, W., Zhu, R., & Tu, Z. (2022). Modeling and thermal management of proton exchange membrane fuel cell for fuel cell/battery hybrid automotive vehicle. *International Journal of Hydrogen Energy*, 47(3), 1888-1900. https://doi.org/10.1016/j.ijhydene.2021.10.146.

[6] Abdalla, S. A., Abdullah, S. S., & Kassem, A. M. (2022). Performance enhancement and power management strategy of an autonomous hybrid fuel cell/wind power system based on adaptive neuro fuzzy inference system. *Ain Shams Engineering Journal*, 13(4), 101655. https://doi.org/10.1016/j.asej.2021.101655.

[7] Jouili, Y., Youssef, M. A. B., Hamed, B., & Sbita, L. (2021, October). Brushless DC motor fed by PEM fuel cell stack for mini UAV's. *In 2021 12th International Renewable Energy Congress (IREC) (pp. 1-6). IEEE*. https://doi.org/ 10.1109/IREC52758.2021.9624822

[8] REDDY, H., & SHARMA, S. (2021). Implementation of Adaptive Neuro Fuzzy Controller for Fuel Cell Based Electric Vehicles. *Gazi University Journal of Science*, 34(1), 112-126. https://doi.org/10.35378/gujs.698272.

[9] Kumar, K., Tiwari, R., Varaprasad, P. V., Babu, C., & Reddy, K. J. (2021). Performance evaluation of fuel cell fed electric vehicle system with reconfigured quadratic boost converter. *International Journal of Hydrogen Energy*, 46(11), 8167-8178. https://doi.org/10.1016/j.ijhydene.2020.11.272

[10] Vasantharaj, S., Indragandhi, V., Subramaniyaswamy, V., Teekaraman, Y., Kuppusamy, R., & Nikolovski, S. (2021). Efficient Control of DC Microgrid with Hybrid PV—Fuel Cell and Energy Storage Systems. *Energies*, 14(11), 3234. https://doi.org/10.3390/en14113234

[11] Harrag, A., & Rezk, H. (2021). Indirect P&O type-2 fuzzy-based adaptive step MPPT for proton exchange membrane fuel cell. *Neural Computing and Applications*, 33(15), 9649-9662.

[12] Lu, P., Huang, W., & Xiao, J. (2021, June). Speed tracking of Brushless DC motor based on deep reinforcement learning and PID. *In 2021 7th International Conference on Condition Monitoring of Machinery in Non-Stationary*

Operations (CMMNO),(pp. 130-134). IEEE. DOI: 10.1109/CMMNO53328.2021.9467649.

[13] [Yamina, J. M., Garraoui, R., & Mouna, B. H. (2020, July). Pem Fuel Cell With Conventional MPPT. In 2020 17th International Multi-Conference on Systems, *Signals & Devices (SSD*) (pp. 249-255).IEEE. DOI: 10.1109/SSD49366.2020.9364218.

[14] Song, B., Xiao, Y., & Xu, L. (2020). Design of fuzzy PI controller for brushless DC motor based on PSO–GSA algorithm. *Systems Science & Control Engineering*, 8(1), 67-77. https://doi.org/10.1080/21642583.2020.1723144 .

[15] Mahmood, R. S., Shabbir, G., Khan, H. U., Mahmood, R. B., Ahmad, S., & Riaz, Z. (2021, December). Speed Control of Brushless DC Motor with Oustaloup Fractional-Order Proportional Integral Derivative FOPID. *In 2021 16th International Conference on Emerging Technologies (ICET*) (pp. 1-5). IEEE. DOI: 10.1109/ICET54505.2021.9689833

[16] Derbeli, M., Barambones, O., Silaa, M. Y., & Napole, C. (2020, October). Real-time implementation of a new MPPT control method for a DC-DC boost converter used in a PEM fuel cell power system. *In Actuators* (Vol. 9, No. 4, p. 105). MDPI.https://doi.org/10.3390/act9040105

[17] Napole, C., Derbeli, M., & Barambones, O. (2021). Fuzzy Logic Approach for Maximum Power Point Tracking Implemented in a Real Time Photovoltaic System. *Applied Sciences*, 11(13), 5927. https://doi.org/10.3390/app11135927

[18] Song, B., Xiao, Y., & Xu, L. (2020). Design of fuzzy PI controller for brushless DC motor based on PSO–GSA algorithm. *Systems Science & Control Engineering*, 8(1), 67-77. https://doi.org/10.1080/21642583.2020.1723144

[19] Derbeli, M., Barambones, O., Farhat, M., Ramos-Hernanz, J. A., & Sbita, L. (2020). Robust high order sliding mode control for performance improvement of PEM fuel cell power systems. *International Journal of Hydrogen Energy*, 45(53), 29222-29234. https://doi.org/10.1016/j.ijhydene.2020.07.172.

[20] Khaniki, M. A. L., Esfandiari, S., & Manthouri, M. (2020, October). Speed Control of Brushless DC motor using Fractional Order Fuzzy PI Controller Optimized via WOA. In 2020 10th *International Conference on Computer and Knowledge Engineering (ICCKE)* (pp. 431-436). IEEE. https://doi.org/10.1109/ICCKE50421.2020.9303634.

[21] Yigit, T., & Celik, H. (2020). Speed controlling of the PEM fuel cell powered BLDC motor with FOPI optimized by MSA. *International Journal of Hydrogen Energy*, 45(60), 35097-35107. https://doi.org/10.1016/j.ijhydene.2020.04.091

[22] Gadekar, K., Joshi, S., & Mehta, H. (2020, July). Performance Improvement in BLDC Motor Drive Using Self-Tuning PID Controller. *In 2020 Second International Conference on Inventive Research in Computing Applications (ICIRCA*) (pp. 1162-1166). IEEE. DOI: 10.1109/ICIRCA48905.2020.9183219

[23] Suryoatmojo, H., Pratomo, D. R., Soedibyo, M. R., Riawan, D. C., Setijadi, E., & Mardiyanto, R. (2020). Robust speed control of brushless dc motor based on adaptive neuro fuzzy inference system for electric motorcycle application. *International Journal of Innovative Computing Information and Control*, 16(2), 415-428

[24] Devi Vidhya, S., & Balaji, M. (2020). Hybrid fuzzy PI controlled multi-input DC/DC converter for electric vehicle application. *Automatika*, 61(1), 79-91. https://doi.org/10.1080/00051144.2019.1684038 .

[25] Parvathy, T. S., & Abraham, P. K. (2020, April). Fast response antiwindup self tuning fuzzy PID speed control of brushless DC motor drive. *In AIP Conference Proceedings* (Vol. 2222, No. 1, p. 040014). AIP Publishing LLC. https://doi.org/10.1063/5.0004192

[26] Reddy, K. J., & Sudhakar, N. (2019). ANFIS-MPPT control algorithm for a PEMFC system used in electric vehicle applications. *International Journal of Hydrogen Energy*, 44(29), 15355-15369. https://doi.org/10.1016/j.ijhydene.2019.04.054

[27] Verma, V., & Chauhan, S. (2019, June). Adaptive PID-fuzzy logic controller for brushless DC motor. In 2019 3rd International Conference on Electronics, *Communication and Aerospace Technology (ICECA)* (pp. 445-449). IEEE. DOI: 10.1109/ICECA.2019.8821941

[28] Hu, H., Wang, T., Zhao, S., & Wang, C. (2019). Speed control of brushless direct current motor using a genetic algorithm–optimized fuzzy proportional integral differential controller. *Advances in Mechanical Engineering*, 11(11), 1687814019890199. https://doi.org/10.1177/1687814019890199

[29] SARIKAYA, M. S., & DERDİYOK, A. (2019, October). Speed Control of Brushless Direct Current Motor with Fuzzy Resetting Rate PI Controller. *In 2019 3rd International Symposium on Multidisciplinary Studies and Innovative Technologies (ISMSIT)* (pp. 1-4). IEEE.

[30] Tahoun, A. H. (2017). Anti-windup adaptive PID control design for a class of uncertain chaotic systems with input saturation. ISA transactions, 66, 176-184.

[31] PILAKKAT, S. et KANTHALAKSHMI, S. Study of the Importance of MPPT Algorithm for Photovoltaic Systems under Abrupt Change in Irradiance and Temperature Conditions. *WSEAS Trans. Power Syst*, 2020, vol. 15. DOI: 10.37394/232016.2020.15.2

[32] Derbeli, M., Farhat, M., Barambones, O., & Sbita, L. (2017). Control of PEM fuel cell power system using sliding mode and super-twisting algorithms. *International journal of hydrogen energy,* 42(13), 8833-8844. https://doi.org/10.1016/j.ijhydene.2016.06.103.

[33] Agrawal, S., & Shrivastava, V. (2017, July). Particle swarm optimization of BLDC motor with fuzzy logic controller for speed improvement. *In 2017 8th International Conference on Computing, Communication and Networking Technologies (ICCCNT*) (pp. 1-5). IEEE. DOI: 10.1109/ICCCNT.2017.8204006

Contribution of Individual Authors to the Creation of a Scientific Article (Ghostwriting Policy)

The authors equally contributed in the present research, at all stages from the formulation of the problem to the final findings and solution.

Sources of Funding for Research Presented in a Scientific Article or Scientific Article Itself

No funding was received for conducting this study.

Conflict of Interest

The authors have no conflicts of interest to declare that are relevant to the content of this article.